

# Multiple Streamline Tractography Approach with High Angular Resolution Diffusion Imaging Data

Y-P. Chao<sup>1</sup>, C-H. Yeh<sup>2</sup>, K-H. Cho<sup>1</sup>, J-H. Chen<sup>1</sup>, and C-P. Lin<sup>3</sup>

<sup>1</sup>Institute of Electrical Engineering, National Taiwan University, Taipei, Taiwan, <sup>2</sup>Institute of Radiological Sciences, National Yang-Ming University, Taipei, Taiwan, <sup>3</sup>Institute of Neuroscience, National Yang-Ming University, Taipei, Taiwan

## Introduction

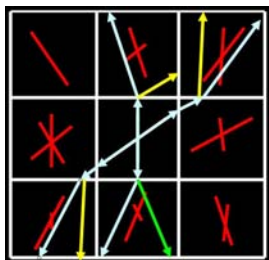
Knowledge of brain connectivity between neural histoarchitecture is requested to the understanding of brain function. Recent advanced diffusion MRI can non-invasively map neuronal architecture by probing diffusivity of water molecules in brain structure and thus can reveal complex neuronal orientations in human brain [1]. Numerical tractography techniques have been developed based on this technique to delineate the white matter pathways by propagating the principle orientation of diffusion tensor and have been applied to clinical diagnosis and the field of neuroscience [2-4]. However, due to the inherent limitation of DTI in mapping multi-fiber orientations within each voxel, the neuronal pathways were most confined to the coherent fiber bundles in human brain [5]. Novel high angular resolution diffusion imaging (HARDI) techniques, such as diffusion spectrum imaging (DSI) and q-ball imaging (QBI) [6, 7], were recently developed to map intravoxel complex dispersions in human brain. In cooperation with these techniques, a new fiber tracking method was developed to map the anatomic connectivity in this study. The results also showed that it could deal with the limitation of DTI in gray matter and reveal complex neuronal architecture from cerebral cortex.

## Materials and Methods

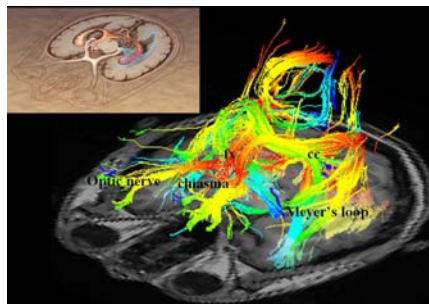
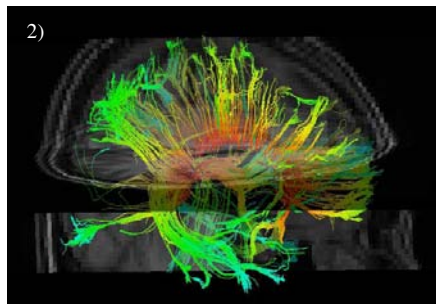
In vivo human QBI data were acquired in a GE Healthcare Signa 1.5T Excite scanner in Taipei Veterans General Hospital by spin echo EPI sequence with 162 icosahedral diffusion-encoding directions, matrix size=128x128, slice number=46, voxel size=2.0x2.0x2.2 mm<sup>3</sup>, TR/TE = 13600/91.2 ms and b<sub>max</sub> = 3000 s mm<sup>-2</sup>. The QBI reconstruction was based on the Funk-Radon transformation [8]. In order to describe the primary fiber components, the 162 symmetric orientations were used for rendering the orientation distribution function (ODF) of each voxel. The length in each orientation was regarded as the probability of fiber propagation. The local maximum (local<sub>max</sub>) of ODF was calculated for the request of tracking algorithm. Multiple Fiber Assignment by Continuous Tracking (MFACT) was proposed for constructing 3D human brain neuroanatomical connections in this study. It is similar to the FACT algorithm proposed by Dr. Mori [9] but is practicable for high angular resolution diffusion (HARD) data. In short, it could be described as follows:

1. Set all seed point  $x_i$  as root  $x_r$ , with any local<sub>max</sub> greater than the set threshold
2. Select  $j^{\text{th}}$  orientation of the local<sub>max</sub>  $v_j$  at  $x_r$  as the current direction
3. Calculate the next point  $x_{ij}$  of the track on the boundary of this voxel.
4. If the point touches the boundary of the image, go to step 2
5. If each local<sub>max</sub> of the new voxel is less than the set threshold, go to 2
6. Get each angle difference between current  $v_j$  and each orientation of local<sub>max</sub> in the next point.
7. If each angle difference is greater than the set threshold, go to 2
8. Record all  $x_{ij}$  as  $x_i$ , and go to step 1

Fig. 1 shows the tracking schematic diagram. The seed point is selected in the center. The tracts are then propagated along the vectors. The yellow tracts indicate the greater angular difference between each step, which might be ignored via threshold setting. The green vector means the local<sub>max</sub> of ODF is less than that of setting threshold. Both thresholds can be adjusted according various study purposes. The algorithm and visualization relied on in-house program developed by Borland C++ Builder 6 and OpenGL API. All tracking results would be stored by tree-structure data format.



▲ Fig.1 The schematic diagram of MFACT approach.



◀ Fig.2 The tracking result of corpus callosum, where seed points were selected from cerebral cortex

◀ Fig.3 The tractography of visual pathway and limbic system by MFACT. fx: fornix cc: corpus callosum

## Results

Fig.2 presents clear neural tracts of corpus callosum from cerebral cortex by MFACT approach [10]. Fig. 3 shows the visual pathway, limbic system, and the corresponding 3D atlas. The optic chiasma and visual cortex (Brodmann's area 17) were assigned as the seed regions with local<sub>max</sub> = 0.7 and the angular threshold = 50°. The color of each point was set from red to blue by the distance between initial seed areas and tract locations. From above results, the tracts were provided with high similarity with known anatomy.

## Conclusions

QBI and other multiple-fiber reconstruction techniques have been implemented for resolving the fiber incoherence problem of DTI recently. In this research, we appraised the appearance of MFACT approach by human brain QBI data with known connectivity. This naive and modified multiple streamline algorithm seems to provide not only white matter connections but also cortico-cortical connection, which is highly correlated to our known knowledge. The primary problem of this method is huge numbers of tracts generated. The combination of Boolean functions, ROI selection, and anatomical knowledge is necessary for further improvement. In summary, MFACT tractography from HARDI could be expected to be a powerful technique on neuroscience study.

## Acknowledgement

This study was supported in part by National Science Council grant (NSC 95-2752-H-010-004-PAE).

## References

- [1] P. J. Basser, et al, *Magn. Reson. Med.*, 44:625-32, 2000. [2] G. J. Parker, et al, *Neuroimage*, 15:797-808, 2002. [3] A. Anwender, et al, *Cerebral Cortex*, 2006. [4] G. J. Parker, et al, *Neuroimage*, 24:656-66, 2005. [5] M. R. Wiegell, et al, *Radiology*, 217:897-903, 2000. [6] D. S. Tuch, *Magn. Reson. Med.*, 52:1358-72, 2004. [7] V. J. Wedeen, et al, *Magn. Reson. Med.*, 54:1377-86, 2005. [8] M. Perrin, et al, *Philos. Trans. R. Soc. Lond. B. Biol. Sci.*, 360:881-91, 2005 [9] S. Mroi and Peter C. M. van Zijl, *NMR in Biomed.*, 15 :468-480, 2002. [10] Y.P. Chao et al., ISMRM 2007 (submitted)